CHAPTER i

Introduction and Literature Review

Chapter index

1 Introduction and Literature Review **3**

1.1 Introduction 3

1.2 The Origin of HPM 5

1.3 Overview and Development of Various HPM Tubes 6

1.3.1 Relativistic Backward Wave Oscillator (RBWO) 6

1.3.2 Relativistic Magnetron (RM) 7

1.3.3 Relativistic Klystron Amplifier (RKA) and, Relativistic Klystron Oscillator (RKO) 9

1.3.4 Magnetically Insulated Line Oscillator (MILO) 11

1.3.5 Split Cavity Oscillator (SCO) 14

1.3.6 Transit-Time Oscillator (TTO) 15

1.3.7 Plasma Assisted Slow-wave Oscillator (PASOTRON) 16

1.3.8 Arletron 17

1.4 Literature Review on Reltron 18

1.4.1 Time-line of reltron deveopment 19

1.4.2 Literature review 21

1.4.3 Standpoint of Reltron 29

1.5 Motivation and Problem Definition 30

1.5.1 Motivation 30

1.5.2 Problem definition 30

1.6 Plan and Scope 31

1.7 Conclusion 32

CHAPTER 1

Introduction and Literature Review

1.1 Introduction

High-Power Microwave (HPM) technology is quite matured and widely used in military and civilian needs. The devices with peak power exceeding 100 MW and frequency ranging from 1 to 300 GHz come under the broad category of HPM. One major application of this technology is non-lethal Directed Energy Weapons (DEWs). The HPM radiation can be produced by various microwave tubes. In general, electron gun emits the beam, which is guided through the tube's RF interaction structure. As the beam interacts with the RF fields, it losses a net kinetic energy, which eventually converts into microwave radiation. Three kinds of radiation take place in HPM sources, depending on the nature of beam field interaction –

- Cherenkov radiation,
- Bremsstrahlung radiation,
- Transition radiation.

Cherenkov radiation occurs when the electrons move through a high refractive index medium ($n = c/v > 1$), so that the phase velocity of electromagnetic waves ($v_{ph} = c/n$) is less than electrons velocity (v). This happens in linear beam devices (travelling-wave

tubes (TWTs), backward-wave oscillators (BWOs)), and cross-field tubes (magnetron, magnetically insulated line oscillator (MILO)). These devices can produce several GWs of power with a pulse length of 10-100 ns at the frequency range of 1-10 GHz and pulse repetition rates of a few hundreds of Hz.

When electrons oscillate in externally applied – constant or periodic, magnetic and/or electric field, Bremsstrahlung radiation occurs. The frequency of electromagnetic radiation matches with either the Doppler-shifted oscillation frequency of electrons or with its harmonics. The oscillation happens in the presence of – periodic and constant magnetic fields in free-electron lasers (FELs) and cyclotron resonance masers (CRMs), respectively. These devices are inherently tunable, and broadband and their frequency range exceed 100 GHz. They can be operated in continuous wave (CW) mode. Gyrotron is an example of such a device with the highest average power output.

Transition radiation occurs when electrons traverse through two different media, or some metallic grids or plates. Relativistic klystron oscillator (RKO), relativistic klystron amplifier (RKA), and the Reltron are some examples. These devices can produce power exceeding 10 GW with $\sim$100 ns pulse durations near 1 GHz frequency. The single-shot devices produce the highest power.

Apart from the above three classes, the virtual cathode oscillator (VIRCATOR) [Sullivan *et al.* (1983)] is a specialized HPM source. Here, the microwave radiation is not generated from the beam wave interaction. A virtual cathode is formed as the potential energy of the space charge in the electron beam becomes higher than the beam's kinetic energy. VIRCATORs can be built in three geometrical configurations – axial, coaxial, and reflex triode [Davis *et al.* (1990)]. After a virtual cathode is formed due to the depressed electrostatic potential, it makes some electrons to flow in the reverse direction. As a result, the electrons reflex back and forth between the virtual cathode and the actual cathode. Two kinds of radiation happen here – i) the virtual cathode itself oscillates with plasma frequency, and ii) the reflexing electrons oscillate at some other frequency. Though VIRCATORs do not require a magnetic field and have a relatively simple and compact design, their biggest drawback is very poor efficiency, as the two competitive radiations

do not occur at the same frequency. However, phase and frequency locking have been demonstrated [Price *et al.* (1989)], [Sze *et al.* (1990)]. VIRCATORs have output power exceeding 1 GW in L and S-band with an efficiency of less than 10%. Virtual cathodes may be formed periodically in reltron's modulation section during the peak of bunching. Depending on the average or peak output power and mode of operation, the HPM sources can be divided into two categories–

- high average power sources (with high-repetition-rate, and long-pulse duration or continuous wave devices),
- high-peak-power sources (with low-repetition rate, and short-pulse duration or "single shot" devices).

Examples of state-of-the-art devices in the above two categories are – the 150 MW, 2.998 GHz klystron at Stanford Linear Accelerator Center (SLAC), Menlo Park, California, and 2 GW, 1.2 GHz (pulse duration <200 ns) MILO at the Air Force Research Laboratory (AFRL), Kirtland AFB, New Mexico, respectively [Benford *et al.* (2007)].

1.2 The Origin of HPM

The present HPM technology is an assemblage of several inventions and successive developments. Klystron was developed in 1937, which is the first cavity-type microwave device. During World War-II (1939-1947), the rapid development of magnetron and the invention of TWT and the BWO took place. The requirement for a higher average power source at over 100 GHz frequency for controlling thermonuclear fusion, led to the development of gyrotrons during the 1950s. The cross-field amplifiers (CFAs) were developed during the 1960s. During the same time, advancement in electrical technology led to the realization of beams with high currents and voltages (exceeding 10 kA and 1 MV, respectively). This intense relativistic electron beams (IREBs) translated the existing tube technology into the relativistic regime, and devices like relativistic backward wave oscillator (RBWO), relativistic magnetron (RM), relativistic klystron amplifier (RKA), and

relativistic klystron oscillator (RKO) were developed. Plasma assisted devices, reltron, and arletron are the latest addition to the HPM family [Benford *et al.* (2007)].

1.3 Overview and Development of Various HPM Tubes

A brief description of various HPM sources and their stepwise development are briefly described below.

1.3.1 Relativistic Backward Wave Oscillator (RBWO)

BWOs amplify the waves propagating in the backward direction with respect to the electron beam. The beam interacts with the first order spatial harmonic of the backward wave. A cutoff waveguide at the cathode side reflects the backward wave, and the output is collected from the other end. This reflected wave does not take part in synchronous interaction with the electron beam. By altering the operating voltage and/or the structure period, the operating point can be shifted to any point on the region with the negative slope of the dispersion diagram, lying below the light line.

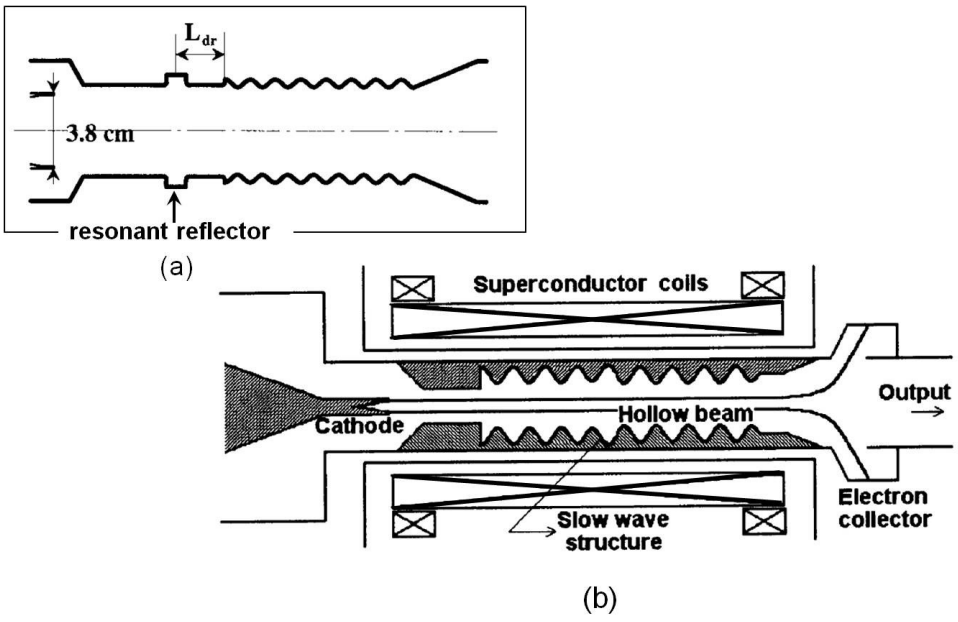

Figure 1.1: Schematic diagram of RBWO (a) with resonant reflector [Guinn *et al.* (1998)], and (b) with electron collector [Chen *et al.* (2002)].

The RBWOs operate at a higher voltage and current level. They have undergone signifi-

cant research activities for more than three decades leading to considerable advancement and a better understanding of the device. Some notable developments are – i) enhancing the tuning range by varying the length of smooth wall waveguide, [Moreland *et al.* (1996)], ii) improving output power and efficiency by pre-bunching the electrons using resonant reflector (Figure 1.1(a)) [Gunin *et al.* (1998)], iii) use of non-uniform slow-wave structure (SWS) to improvement the efficiency further [Wen *et al.* (2000)], iv) operation at 100 Hz repetition rate with 1.1 GW of power at 9.38 GHz by using specially designed electron beam collector (Figure 1.1(b)) [Chen *et al.* (2002)] v) use of two uniform SWSs separated by a drift tube to increase the velocity modulation [Zhang *et al.* (2004)], vi) using two RRs to increase the pulse length [Song *et al.* (2011)] and, vii) use of trapezoidal resonant reflector for shifting the peak electric field towards the center of the RR for reducing the probability of RF breakdown [Cao *et al.*(2014)].

1.3.2 Relativistic Magnetron (RM)

During World War II, magnetrons were produced on a very large scale, "and magnetron-driven radar probably had a greater impact on the war than any other technology invented in World War II, more so than even the atomic bomb." Magnetrons are a cross-field device, where the applied axial magnetic field is perpendicular to the DC electric field along the anode-cathode gap. The electrons drift with a velocity close to v_{ph} of the slow electromagnetic wave in the interaction region. For cylindrical magnetron, the operating voltage is governed by Buneman–Hartree resonance condition, and the Hull cutoff condition gives the range of the magnetic field. The relativistic magnetron (RM) is an extrapolation of the cavity magnetron in terms of voltage and current. RMs are driven by a pulsed power supply that makes the cold cathode to emit high current and employ different output extraction techniques that allow the electron beam to be collected in a larger area collector. The first RM was a six-vane (A6), single-shot, uncooled device with radial extraction that produced 1.7 GW power at 3 GHz frequency with 35% efficiency and had a pulse duration of 30 nS [Bekefi *et at.* (1976)]. The principal thrust area was to generate higher RF energies by broadening the pulse durations and increasing the average power. In

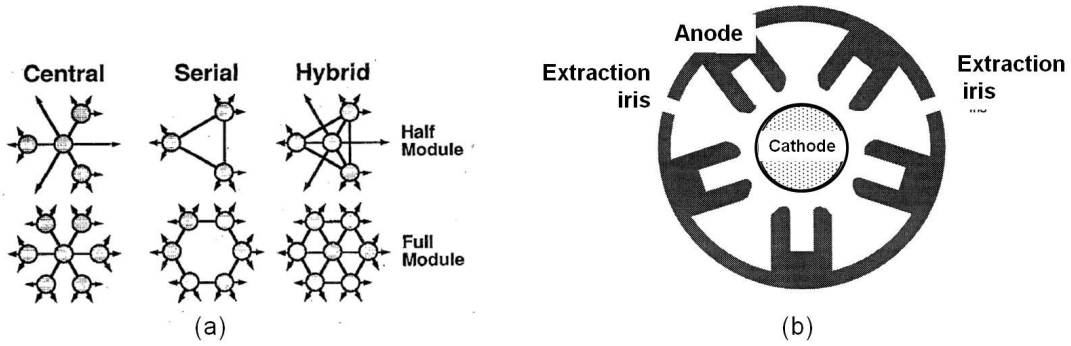

Figure 1.2: (a) Interconnection geometries of phased locked RM [Levine *et al.* (1991)], and (b) frequency-agile RM (RS10) [Levine *et al.* (1995)].

magnetron with diffraction output (MDO), instead of extracting the power radially, the anode vanes are tapered axially to the output waveguide by a smooth and continuous transition. This increased the interaction length region without disturbing single-mode operation. Subsequently, the current can be increased nearing the cutoff condition, resulting in a power of 4 GW with 0.95 MW applied voltage and 9.2 GHz frequency [Kovalev *et al.* (1977)]. A similar output couping technique, combined with the use of "Washer" cathode in A6 magnetron reached 6.9 GW of power (1.15 GW per waveguide) at 4.5 GHz [Benford *et al.* (1985)]. Once the highest power from an individual source was achieved, multiple sources were combined to form coherent array to achieve even higher magnitude of radiated powers. Two techniques are used for the phase locking of multiple magnetrons – i) peer-to-peer (P2P) or ii) master-to-slave (M2S). In P2P, the output ports are connected to a common external load. Whereas in M2S operation, higher-power slave oscillators are driven by a low-power master oscillator. Four and seven RMs were connected in central, serial, and hybrid configuration through phase-locking (Figure 1.2(a)), and the whole module produced 2 GW with four and 2.9 GW with seven magnetrons at 2.8 GHz [Levine et al. (1991)]. Frequency tunability was achieved over a broad band at output power 400 to 600 MW rising sun structure (RS10) having alternating rectangular cavities and vanes (Figure 1.2(b)). A tuning range of 23.9% and 33.4% from the respective center frequencies of 1.21 GHz and 2.82 GHz was achieved [Levine *et al.* (1995)]. Researchers at the University of New Mexico utilized the transparent cathode, consisting of periodically placed longitudinal emitters along the cathode perimeter in the MDO,

and achieved 70% efficiency in simulations and 63% efficiency in experiments [Fuks and Schamiloglu (2010)]. The transparent cathode had demonstrated higher electronic efficiency, quicker startup, and higher output power than a solid cathode. Magnetic priming [Neculaes *et al.* (2005)] is another technique of hastening the oscillation by imposing an azimuthally varying magnetic field of periodicity N/2, (N being the total cavity numbers). In the cathode priming technique [Jones *et al.* (2004)], the emission area was reduced to three azimuthally periodic regions using projection ablation lithography (PAL). The startup time was reduced by about 50% in both cathode priming and magnetic priming.

1.3.3 Relativistic Klystron Amplifier (RKA) and, Relativistic Klystron Oscillator (RKO)

Klystrons are transition radiation based devices. They can work either in an amplifier or in an oscillator configuration. The interaction structure of a conventional klystron amplifier consists of a fixed buncher cavity and one or more movable catcher cavities. The electron beam traverses from the former to the later through a variable-length drift tube. The buncher cavity segregates a contentious electron beam into bunches by velocity modulation. For producing coherent radiation by decelerating electron bunches in the catcher cavity, the transit angle must not exceed π radians for maintaining the favorable RF phase within the gap length.

The relativistic klystron amplifiers (RKAs) employ an annular beam that can carry higher current (typically 5-20 kA) at the same given voltage than a solid pencil beam, used in conventional klystrons. The RKA was designed at the Naval Research Laboratory (NRL) and has demonstrated 15 GW power at frequency 1.3 GHz having $\sim$50 ns pulse, and $\sim$6 GW power for up to 100 ns pulse in single-shot mode [Friedman *et al.* (1990)]. The beam space charge plays an important role in RKA operation, and a single buncher cavity can produce a beam bunching with 1.5 times more current in the fundamental harmonic than the DC current. This high degree of modulation was due to electrons reflexing from virtual-cathodes within the cavities [Friedman *et al.* (1984)]. There are a few shortcomings of RKA like – i) lower output power and efficiency at a higher frequency, and ii)

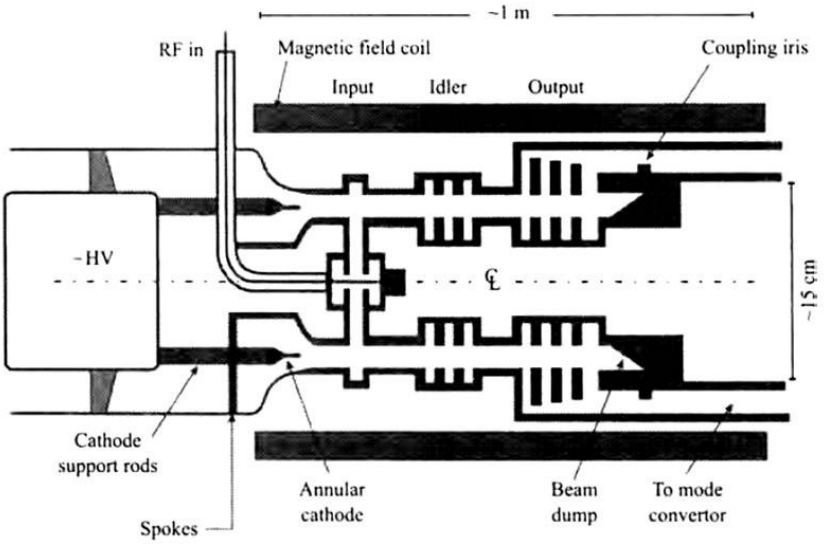

Figure 1.3: Schematic diagram of tri-axial RKA [Friedman *et al.* (1993)].

limitation on pulse duration as well as repetition rate due to its beam interception mechanism. To overcome the shortcomings, a triaxial version of RKA was envisioned where an annular beam propagates between two coaxial conductors [Friedman *et al.* (1993)]. This configuration allows about twice current in comparison with the original RKA and requires a lower magnetic field for beam confinement. The combination of higher current and larger volume resulted in a substantial increase in operating power.

The Friedman RKA was converted to a self-oscillating variant known as the relativistic klystron oscillator (RKO) by introducing a feedback mechanism involving electromagnetic coupling between the cavities rather than reflecting the beam, and by using a tri-axial extractor. This device demonstrated 1.5 GW of power [Hendricks *et al.* (1996)].

Depending on the operational features the relativistic klystrons can be divided into three types – i) high-impedance near-relativistic klystrons; the 2.6 m long, 300 kg klystron made by SLAC for DESY (Deutsches Elektronen-Synchrotron) with 535 kV beam voltage, 700 A beam current, 150 MW output power at 2.998 GHz frequency. The efficiency was 40%, and it required 15 kW additional power to produce a 0.21 T magnetic field through solenoidal coil [Sprehn *et al.* (1994)]. Later, periodic permanent magnet (PPM) focusing was used to save power, spend on electromagnet [Sprehn *et al.* (1996)]. ii) High-impedance relativistic klystrons; the 250 MW SL-4 multi-output klystron with 1.3

MV voltage, and 520 A RF current [Allen *et al.* (1989)]. iii) Low-impedance klystron; the annular-beam klystron at NRL with 500 kV, 5 kA input, and 1.7 GW output power at frequency 3.5 GHz [Friedman *et al.* (1988)].

1.3.4 Magnetically Insulated Line Oscillator (MILO)

The magnetically insulated line oscillator (MILO) is a linear variant of magnetron that takes benefit of the high current capability of advanced pulsed power supply. MILOs can have either planner or coaxial geometry. In a coaxial MILO, one end of the inner conductor functions as the cathode, and suspended metal discs from the outer wall function as SWS. The outer conductor also works as the outer wall of the extraction section. The high current emitted from the cold cathode generates an axial magnetic field, restraining the beam from reaching the anode before RF interaction. The beam drifts axially through a layer close to the cathode surface under the influence of this magnetic insulation. When the drift velocity of the electrons is close to the phase velocity of an electromagnetic wave in the SWS, Brillouin flow resonates with the wave, and the wave grows by taking energy from the electrons. The advantage of the MILO is low impedance that makes it compatible with low-impedance pulsed power supplies like explosive flux compression generators or waterlines.

The initial experimental work reported about 50 MW of power with < 75 nS pulse duration that used more numbers of cavities ($\geq$6), and radial power extraction through irises cut in cavity walls [Clark et al. (1988)]. The realization of axial extraction was a major discovery that achieved 300 MW power for a short pulse of 10 nS [Lamke et al. (1990)]. The uniform cavity MILOs suffered from leakage of microwaves towards the pulsed power source, that returned at a wrong phase after reflection, making a significant reduction in power. To eliminate the problem, two leftmost cavities were made deeper than the main SWS cavities (chokes). Implementation of microwave choke increased the feedback to the SWS, enhancing efficiency. By decreasing the vane length of the last SWS cavity resulted in a better impedance matching between the MILO and output transmission line (beam dump), improving the output power. Redesigning the beam dump to isolate it from

the microwave extractor and chokes' addition improved the power to 1.5 GW. Still, the design suffered from severe pulse shortening with a microwave pulse of only 70 nS for a 500 nS beam pulse [Calico *et al.* (1995)]. Later, the number of cavities in SWS was minimized that eliminated azimuthally symmetric mode competition [Lamke *et al.* (1997)]. In an all-stainless-steel brazed MILO (*hard-tube* MILO-HTMILO), cathode tapering was used to eliminate unwanted emission from the bare stainless steel cathode region under the choke section that demonstrated 2 GW power with 175 nS pulse length, that was almost equal to the pulse duration of driving supply [Haworth *et al.* (1998)]. *Tapered* MILO was proposed to overcome the difficulty in extracting energy from MILO operating in π-mode having zero group velocity [Eastwood et al. (1998)]. It employs a driver section with three cavities for beam bunching in π-mode, followed by a gentle, and a sharp taper sections. The group velocity is of gradually increasing order in the last two sections for propagating more energy out of the interaction region, without hindering the coupling between the drifting electrons and the interaction structure. An improved MILO was reported in 2007. The simulation predicted 4.24 GW power at 1.76 GHz, with input voltage and current of 600 kV and 52 kA, respectively. This improvement was a collective effect of – i) a movable beam dump disc, capable of easy optimization of the magnetic field, by changing the load current, ii) reduced number of cavities in RF choke section from two-cavity to one-cavity, resulting in a more compact design while offering 99.4% reflection of the leaking RF power (0.5% less than two-cavity choke section), and iii) using a novel high-power mode-transducing antenna, that efficiently converts the TEM wave into the TE_{11} mode, and then radiates from a coaxial horn antenna into the air [Fan *et al.* (2007)]. *Bifrequency* MILO (BFMILO) was proposed in 2009 that used azimuthal partition of the cavity depth for generating HPM in two frequencies from a single device (Figure 1.4(a)). Simulation results predicted 1.3 GW power with efficiency of $\sim$8.1%. in two frequencies 1.27 and 1.49 GHz with input current of $\sim$38 kA and voltage of 420 kV [Chen *et al.* (2009)]. Dwivedi and Jain derived the dispersion relation of a disk loaded coaxial structure same as MILO in various TM modes using field matching technique [Dwivedi and Jain (2012)], and published the design methodology, and parameter optimization

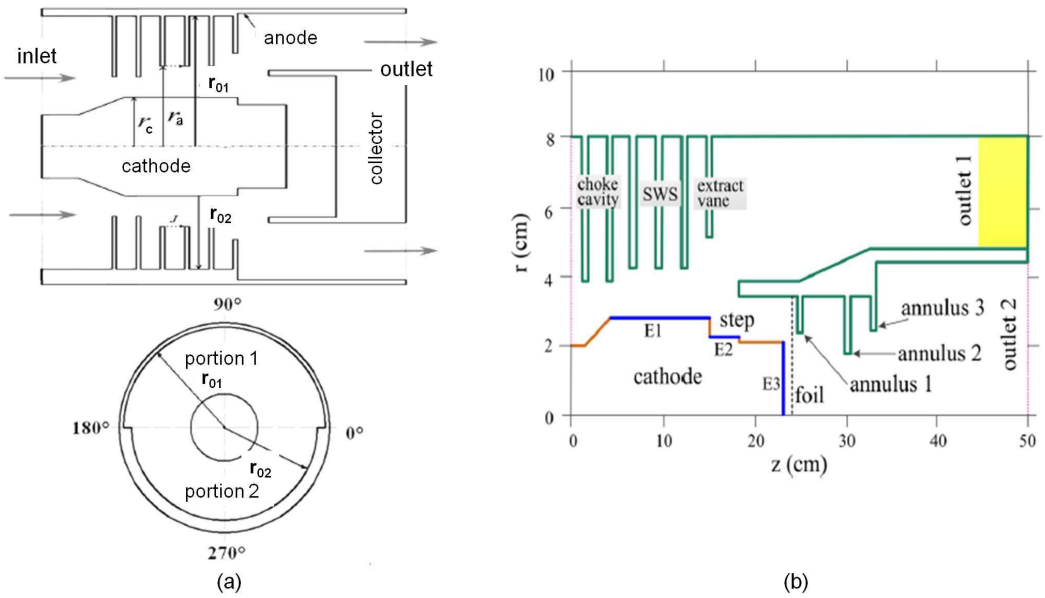

Figure 1.4: MILO in (a) bifrequency configuration [Chen *et al.* (2009)], and (b) a dual-band HPM source [Zhang et al. (2015)].

study of the output power and efficiency, with respect to various design parameters for S-band MILO [Dwivedi and Jain (2013)]. Performance improvement of tapered MILO by impedance matching technique has reported 11.78%, 11%, and 20% improvement in total efficiency, conversion efficiency, and extraction efficiency than in the unmatched case with 15.5%, 21%, and 73%, respectively [Dwivedi and Jain (2014)]. Zhang *et al.* demonstrated a novel concept of driving a C-band virtual cathode oscillator by the load current of a MILO in S-band, to have a dual-band HPM source in the same device (Figure 1.4(b)) that achieved an overall efficiency of 13.4%. The MILO produced 1.70 GW at 2.1 GHz with 10.6% efficiency, and the vircator produced 0.37 GW at two frequencies 4.1 GHz and 3.8 GHz when supplied with an input of 440 kV and 35 kA [Zhang et al. (2015)]. In recent years, a performance improvement study was reported that employed an equivalent circuit approach for matching the impedance between successive sections. With optimized parameters this study has reported an improved efficiency of 14.4% from the reference work with efficiency of 7.8% [Kumar *et al.* (2019)]

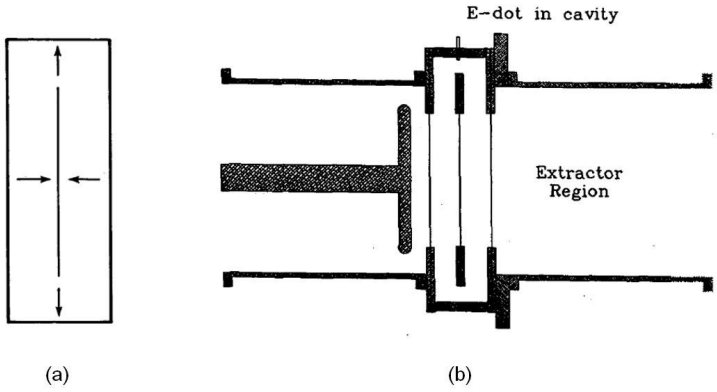

Figure 1.5: SCO (a) fundamental mode, and (b) schematic of experiment [Marder *et al.* (1992)].

1.3.5 Split Cavity Oscillator (SCO)

In a split cavity oscillator (SCO), a pillbox cavity is symmetrically divided into two pillboxes by a conducting screen, through which an electron beam can travel with a minimal interception (Figure 1.5). The screen is placed in such a way that a gap remains between the screen and the cavity outer-wall. This configuration gives rise to a new category of cavity modes in the interaction region, along with the conventional modes. The fundamental mode of this new kind (the SCO mode) grows in amplitude through unstable interaction with a traversing electron beam by taking its kinetic energy. At saturation, the field amplitude becomes adequately large to bunch a traversing beam. Thus, it fully modulates a large cross-section beam within a small distance without any focusing arrangement, overcoming the space-charge and pinching limitations [Marder *et al.* (1992)]. The SCO was developed from the need of a long pulse microwave tube with high power capability. The two needs were accomplished successfully with long pulse duration (typically 1 μS), and achievable phase-locking of several oscillators to attain high total power.The simulation result shows, for an applied voltage, if the beam current is much lower than the Child-Langmuir current, the oscillation is weak and dominated by the second harmonic. For fundamental mode operation, the screen spacing should cause approximately the same emission as the Child-Langmuir current. The bunched beam is collected by an inverse diode that forms a coaxial transmission line with the extended outer wall

of the interaction section. The microwave is extracted from an iris opening, that converts the coaxial transmission line into a cavity with suitable Q and resonant frequency. The positioning of the iris is crucial for successful extraction. Other than pillbox, SCOs can be designed in an elongated or annular shape. The SCOs can operate with 100-300 kV voltage, and their impedance ranges from 50-100Ω. Experiments demonstrated 25 MW of average radiated power with 8% efficiency (nearly twice peak power and efficiency) over 800 nS pulse duration. The efficiency can be enhanced by using the postacceleration technique, and the power can be improved by using annular beams with a large area, or by phase-locking multiple devices. Phase-locking of up to 5 SCOs was successfully achieved.

1.3.6 Transit-Time Oscillator (TTO)

An electron beam excites and enhances suitable electromagnetic modes while it axially transits through a high Q cylindrical cavity. This effect is used to generate microwaves in a transit-time oscillator.

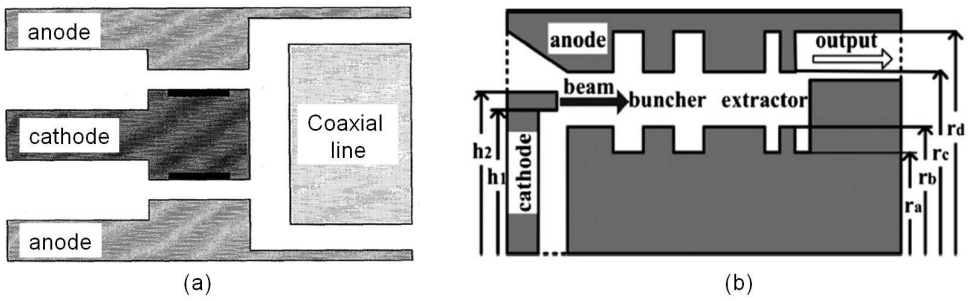

Figure 1.6: Schematic diagram of (a) radial acceleretron [Arman (1996)], and (b) low-impedance TTO (LITTO) [Cao *et al.* (2009)].

Müller proposed transit-time effect based device monotron in 1933 [Müller (1933)]. The device suffered from a low growth rate and extremely poor efficiency due to the nonavailability of relativistic beam technology at that time. Research in this field was abandoned due to the technological imitation for almost six decades. The 20% efficiency in SCO [Marder *et al.* (1992)] was a significant achievement in TTO development. But, the input beam power was limited due to high diode impedance (∼100Ω), restricting the output

power. The transit-time amplifier was proposed in 1993 as a high-efficiency narrow-band device requiring a low magnetic field (0.5 KG), and simulation predicted approximately 1 GW power in X-band [Arman *et al.* (1993)]. The radial acceleretron was developed (Figure 1.6(a)) as a low impedance ($\sim$25Ω), repetitively pulsed device with high power capability. The simulation predicted 1 GW output power with 50% efficiency [Arman (1996)]. The disadvantages of this device were long saturation time and difficulty in extracting output. A more promising low-impedance TTO (LITTO) was proposed in 2009 that employed annular cathode, coaxial extraction section, and required external magnetic field (Figure 1.6(b)). The interaction structure LITTO is similar to SCO. It uses a dual-cavity extractor section that produces higher current modulation. With 600 kV, 36 kA input, and 0.45 T focusing magnetic field, the low impedance TTO would produce 5 GW at 1.6 GHz frequency with 23.1% efficiency [Cao *et al.* (2009)].

1.3.7 Plasma Assisted Slow-wave Oscillator (PASOTRON)

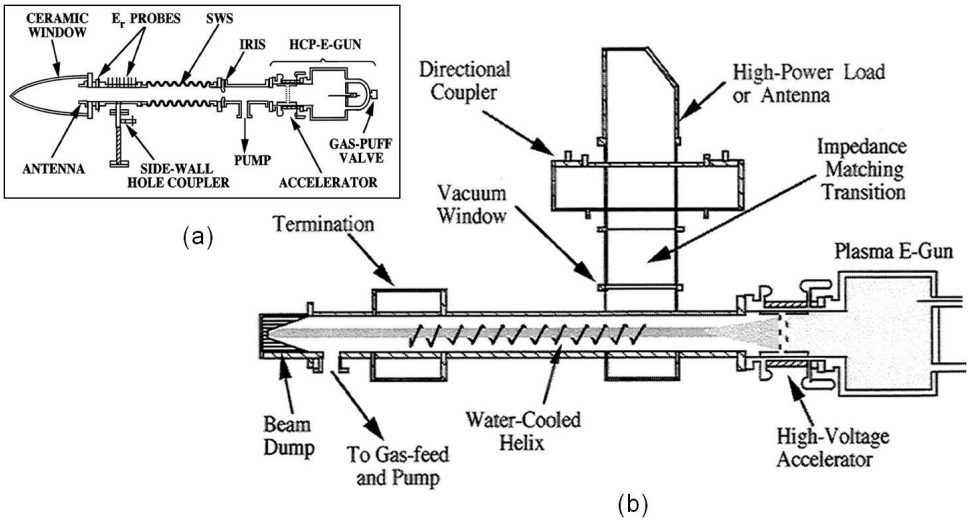

Figure 1.7: Schematic diagram of (a) rippled waveguide SWS PASOTRON, (b) helix-PASOTRON HPM source [Goebel *et al.* (1996)].

Plasma assisted slow-wave oscillator (PASOTRON) employs cylindrical waveguide with a sinusoidaly-varying wall radius as SWS (Figure 1.7(a)), similar to BWOs. A high-perveance plasma-cathode electron gun creates a plasma that works as a high-density electron source, with up to 220 kV, 2 kA voltage, and current. The beam is neutral-

ized by the space-charge while getting transported in the lightly ionized plasma-channel. Thus, the magnetic self-pinch force becomes adequate to compress the beam, eliminating the need for an external focusing field. PASSOTRON is low weight and compact HPM source that can operate at different frequency bands depending on different SWSs used. The first reported device had a TE_{11} output mode with fixed polarization, while it operates in TM_{01} mode. Also, a rotating polarization in TE mode can be directly produce. It demonstrated long pulse operation (>100 μS) in C-band with output power ranging from 1-5 MW and 20% efficiency [Goebel *et al.* (1994)]. In a later development, PASOTRON was configured to operate as a traveling-wave amplifier in addition to BWO, and 20 MW power in long pulse with nearly 1 kJ energy per pulse was achieved (Figure 1.7(b)) [Goebel *et al.* (1996)]. A mode converter was also designed for feeding power from helix-PASOTRON to high power antenna in TE_{10} mode. Vacuum conditioning and tube surface conditioning are crucial for the desired operation of the device. The vacuum conditioning removes the impurities and excess gas, lengthening the pulse and achieving higher power.

1.3.8 Arletron

Arletron is a compact HPM source that employs a medium power (1 MW) annular beam to produce HPM with a high repetition rate and long pulse duration (Figure 1.8). The interaction structure consists of two pillboxes, coupled through the beam passage aperture. No power is wested in external magnetic coils, as permanent magnets can provide the required small focusing field. The device uses the postacceleration technique to enhance the output power and to reduce the energy spread in the bunched beam.

The arletron has demonstrated 350 MW average power at 2.2 GHz with 35% efficiency through simulation. Being a gridless tube, it can operate with a very high repetition rate. It uses tunable plungers to vary the extraction cavity dimension that results in $\pm$25% tunability with respect to the center frequency of 2.4 GHz [Gardelle (2009)]. The dimensions of pillboxes and the beam characteristics limit the design possibility of aretrons within the frequency range of 1-6 GHz. The beam focusing would deteriorate in low-

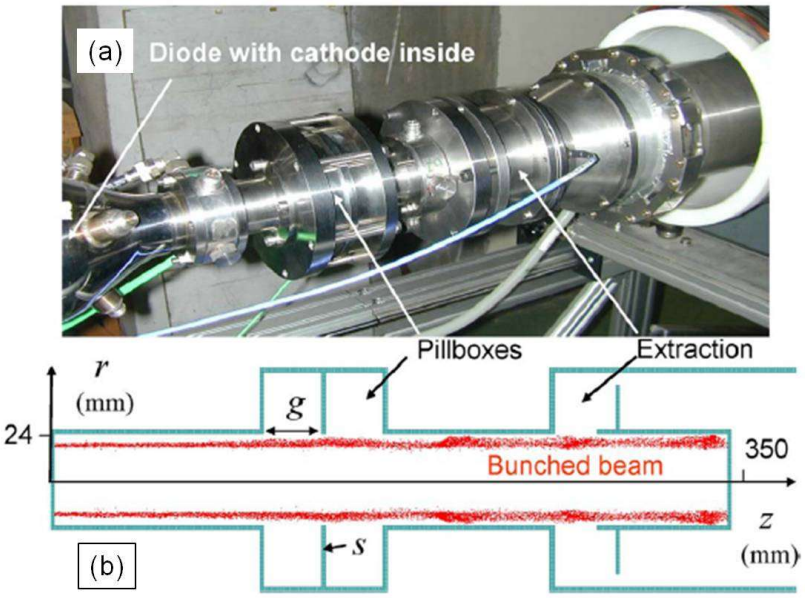

Figure 1.8: Arletron (a) experimental set-up, and (b) MAGIC 3D simulation. [Gardelle *et al.* (2010)].

frequency designs due to insufficient focusing field achievable from permanent magnets. For high-frequency design, the beam current in a small beam dimension would not be sufficiently large for bunching to occur.

In a subsequent work, the simulated design was experimentally tested at Centre d'Etudes Scientifiques et Techniques d'Aquitaine (CESTA), Le Barp, France [Gardelle *et al.* (2010)]. Solid-state pulsed power technology was used in the experiment, providing 1 kA, 200 kV supply with a repetition rate of 100 Hz, and a pulse duration of 300 nS. The generated microwave was radiated by using a TEM to TM_{01} mode converter coupled to a conical horn antenna, and the radiated power was measured at 8 m distance by using S-band horn and detector diode. A good agreement was achieved between the simulated and the experimental works.

1.4 Literature Review on Reltron

Reltrons are a megawatt-class HPM source with high efficiency and excellent frequency stability. These narrowband oscillators do not require magnetic focusing for beam confinement. Reltrons typically use velvet cathodes that are readily available. The pow-

er extraction mechanism is also simple. Figure 1.9 shows the specific energy/pulse × efficiency versus power for a variety of HPM sources. Figure 1.10 shows a schematic diagram of reltron.

Miller *et al.* have invented and developed reltron for more than a decade during the 1990s. They have developed various reltron tubes for HPM effect testing, as well as for educational purpose, and published numerous research articles reporting theoretical analysis, simulations, experimental results, and empirical formulas. Researchers at the University of New Mexico (UNM) have performed experimental and analytical studies on the "UNM Reltron". Indian Institute of Technology (BHU) group have carried out analytical and simulation-based work in recent years. A time-line of research and development on reltron is shown below:

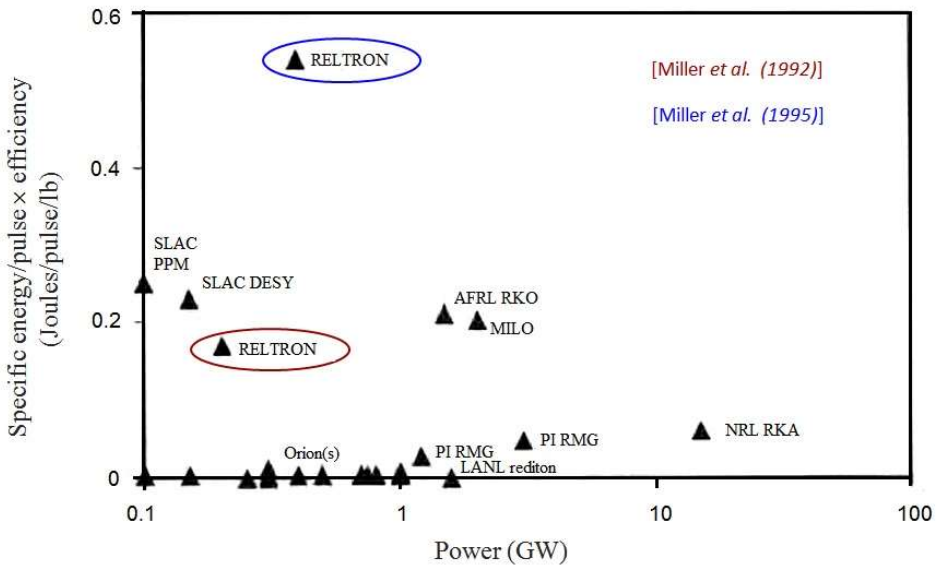

Figure 1.9: Specific energy/pulse × efficiency versus power for a variety of HPM sources [Barker *et al.* (2001)].

1.4.1 Time-line of reltron deveopment

- 1992 → initial development and experiment with 1 GHz, and 3 GHz reltron tubes [Miller *et al.* (1992)].
- 1994 → power enhancement in both tubes, frequency agility (5%) in 3GHz tube, power extraction from higher-order harmonic [Miller *et al.* (1994)].

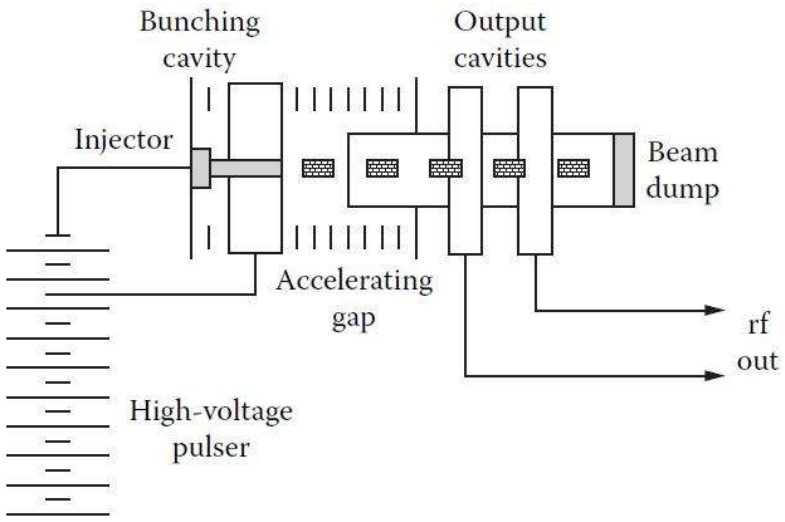

Figure 1.10: Schematic diagram of reltron [Miller *et al.* (1992)].

- 1995 → long pulse operation, extended frequency range, extended lifetime design [Miller *et al.* (1995)].
- 1997 → development of various configurations of reltron compatible pulsed power supplies; analytical description of microwave generation [Miller *et al.* (1997)].
- 1998 → tunability over a wider range (15%), enhanced pulse duration and PRF through velvet cathode; pulse shortening studies [Miller *et al.* (1998)].
- 2001 → cold test (eigenmode simulation, S_{11} measurement), and PIC simulation of an ultra-compact, low voltage reltron, and initial operation its pulsed power system; x-ray shielding requirement [Kenyon (2001)].
- 2002 → full power operation of the pulsed power system, cold test (S_{21} measurement), and initial hot test results [Choi *et al.* (2002)].
- 2009 → PIC simulation of gridless high power reltron with thermionic cathode [Kim *et al.* (2009)].
- 2010 → circuit model of UNM reltron and eigenmode simulation [Soh *et al.* (2010)].
- 2011 → simulation of dual cavity reltron with a power gain of 1.76 [Soh *et al.* (2011)].
- 2012 → dual-mode reltron operation in TM_{010} and/or TM_{110} mode [Soh *et al.* (2012)].
- 2016 → design methodology, and an analytical study on – starting current, oscillation condition, efficiency analysis, bunching field, modulation process, and associated energy, along with PIC simulation [Mahto and Jain (2016)].
- 2017 → analytical study on virtual cathodes formation in reltron [Mahto and Jain (2017)].

- 2019 → simulation study on low impedance reltron [Mahto and Jain (2019)].
- 2020 → simulation study on thermionic emission based reltron [Tripathi *et al.* (2020)].

1.4.2 Literature review

A detailed literature review is summarized below in chronological order. Some abstract papers and publications with redundant experimental results were excluded.

• In the initial work, Miller *et al.* have reported a theoretical summary of super reltron, simulation results of 1D trajectory code and 2D PIC code, and two experiments [Miller *et al.* (1992)]. i) In the 1 GHz reltron experiment, an SCO was used as the modulation section. WR975 waveguides were converted into three output cavities. A shorting plunger terminated one side of each output cavity , and the other side was loaded with inductive iris. Stainless steel wire mesh screens with 90% transparency were used as grids. This experiment produced 400 MW peak power with total input voltage 800 kV and current 1.2 kA giving 41.7% efficiency. The energy per pulse was within the range of 75-85 J. Like in all HPM tubes, pulse shortening was observed. This was examined by using Rogowski coils and B-dot monitors at modulation, and rf output section, respectively. Breakdown in the extraction section was found responsible for the pulse shortening. That was eliminated by widening the iris gap to lower its quality factor. ii) The 3 GHz reltron experiment used a side-couped cavity type modulation section. Output cavities were made of WR340 rectangular waveguide. While operating with the highest voltage, the output power decreased due to RF breakdown in the second extractor. Hence, the quality factors were adjusted to respective values of 20 and 40 for the first and the second extractor. This tube achieved a peak output power of 235 MW with 36.8% efficiency when total input voltage and current were 850 kV and 750 A, respectively.

• Miller *et al.* have published the theoretical calculation of the reactance, the resonant frequency, and the shunt impedance of inductively loaded extraction cavity. The work also included three experiments that demonstrated the power enhancement of the last two tubes, frequency agility of the 3 GHz tube, and possible power extraction in higher harmonics [Miller *et al.* (1994)]. i) In the power enhancement experiment, both tubes

were supplied with higher input power, which made them achieve higher output power. A beam voltage of 250 kV, a postacceleration voltage of 850 kV, and a beam current of 1.35 kA produced 600 MW power with an efficiency of 40.4% in the 1 GHz tube. >200 J energy per pulse was attained. While in the 3 GHz tube, a beam voltage of 200 kV, a postacceleration voltage of 750 kV, and a beam current of 1 kA produced 350 MW power with an efficiency of 36.8%. ii) In the frequency agility experiments, the modulation cavity dimension was varied by tuning screws and plungers. The pulse shape and the power level remained nearly unchanged for multiple shots in fixed-frequency operation, showing consistent nature of the tube. However, the power halved as the frequency was varied to $\pm$5% from the center frequency of 3.04 GHz. iii) In the third experiment, the extraction section of the 3 GHz tube was used for extracting power from the 1 GHz tube. 45 MW power was attained in a long $\sim$1 μS pulse with $\sim$25 J energy per pulse.

• After the initial development, there was a demand for reltron tubes with extended frequency coverage for high power electromagnetic (HPEM) vulnerability testing of electrical systems to HPM pulses. So, the research was focused on three specific topics– long pulse operation, extended frequency coverage, and extended lifetime design. i) For long pulse operation, a new tube was designed at 1.25 GHz frequency with a tuning range from 1.18-1.30 GHz, which can utilize a Marx generator of the same specification as used in 1 GHz and 3 GHz experiments. The tube produced 400 MW power at 1.23 GHz frequency with a typical pulse duration $\sim$200 nS. The gas ionization at the output cavities put a limit to the pulse duration, and approximately 150 J energy per pulse was obtained. ii) An extended frequency range of 1-11 GHz was attained by using interchangeable modulation sections, and additional extraction sections designed for extracting power at second and third harmonics of the fundamental frequency. This system was equipped with stepper motors that can be remotely controlled to select operating frequency during a repetitive pulse operation at 1 Hz. The experimental results show consistent performance with 450 MW peak power in a 100-short burst at 1 Hz repetition rate. iii) For extending the lifetime, klystron inspired design was adopted. In an initial experiment, an existing S-band tube was modified to operate at a lower voltage. This modified design produced 10 MW

power with 1 μS pulse duration and 25 Hz repetition rate. After its success, a 2.856 GHz tube was designed. The tube used a Scandate cathode for achieving a long pulse duration. The operating temperature was 1050^{o}C, and the beam filling factor was 80%. The modulation section was gridless for achieving a longer operating lifetime, and there were two independent output extraction cavities, placed 2π radian phase apart. The vacuum requirement was 10^{-8} torr. This design produced 20 MW output power with 40% efficiency when supplied with 250 kV, 200 A. The typical pulse duration was 5 μS with a repetition rate of 100 Hz. The whole device was 19 inches long and it weighs about 80 pounds, including focusing magnets [Miller *et al.* (1995)].

• In 1997, Miller has published an extensive study of various reltron compatible high-voltage pulsed power supplies. According to the study, the *conventional Marx generator* was suitable for single-shot operation. A crowbar switch was used for terminating the voltage pulse that would otherwise cause late arcing in accelerating gap insulator. Post-acceleration was applied using a divider. The *pulse forming network (PFN) Marx generator* was found suitable for L-band tubes with pulse repetition frequency (PRF) $<$25 Hz, pulse duration within hundreds of nS, rise time $<$100 nS, and a burst of 100 pulses. Here, the post-acceleration was applied by direct tap-off from an intermediate stage. The *transformer-based, repetitively-pulsed modulators* were of two types. a) For tubes with PRF greater than 25 Hz, a thyratron-switched pulse modulator driven step-up transformer (trans ratio 1:12) was suitable. The transformer may produce 260 kV in its secondary winding. This system had an internal resistance of 2.4 kΩ. b) To drive 100 MW, 200 Hz PRF reltron tube, a more sophisticated two-stage driving network was designed. The first stage consisted of a capacitor bank driven pulse transformer, producing 100–150 kV in its secondary winding. This was followed by another HV pulse transformer (ratio 1:8) in the second stage. The secondary winding of this HV pulse transformer could drive a reltron with 500 kV, 500 nS pulses. The rise time of the voltage pulse was kept below 100 nS through a pulse sharpening switch. A resistive divider was used to apply the post-acceleration voltage. The *modulating-anode power supply* was suitable for high average power reltron with output power greater than 100 kW and PRF up to 10 kHz. Empirical

formulas for finding the output power and the diode current were reported. Plots of gun voltage vs. power and impedance for gridded and gridless reltron tubes were also reported. For gridded tubes, the impedance was around 800 Ω, and for gridless tubes, it was 2.5-7.5 kΩ [Miller (1997)].

• Ding has published a physical description of microwave generation via a detailed analysis of beam bunching by exponentially growing and saturated field in modulation cavity. Harmonics of the modulated current was also derived [Ding (1997)].

• Miller *et al.* have reported the progress made in achieving a wider tuning range, lengthening the pulse duration and repetition rate, and increasing the energy per pulse through pulse shortening studies, [Miller *et al.* (1998)]. i) In previous experiments, $\pm 5\%$ tunability was achieved by varying the main cavity dimension using a single-sided tuning plunger. The cylindrical cavity gradually became more rectangular with the withdrawn of the plunger. In theory, this mechanism was able to achieve 29% tunability, but that was not realized in practice. The shift of peak electric field away from the beam axis significantly lowered the beam field interaction over the lower frequency range. So, a two-sided plunger mechanism was used that kept the peak electric field along the axis. This arrangement resulted in a tuning range of $\pm 15\%$ in L-band. ii) Apart from being inexpensive, the velvet cathodes have some other characteristics that are favorable for long pulse operation. It has less plasma velocity (0.25 cm/μS), low threshold electric field ($\sim$16 kV/cm), high emission density (1 kA/cm^2), and they exhibit nearly constant impedance for a considerably long period. It was constructed by adjoining a circular velvet cloth on an aluminum base-plate by using a corona ring. The composites of velvet clothe are 3/4 part rayon and 1/4 part silk. The density varies from 80-250 tufts/cm. A vacuum level of $<10^{-4}$ torr must be maintained for operating without arcing. The erosion rate of 5 x 10^{17} atoms/pulse limits the cathode lifetime to 105 pulses and the PRF to less than 20 Hz, when the pumping speed is 500 l/S. iii) Pulse shortening was extensively studied through experiments. The experimental results revealed that lower transparent grids make lesser pulse shortening, but they decreased the output power. Severe pulse shortening was observed while operating at a higher repetition rate and subsequently, the

vacuum level raised above 10^{-4} torr. Conditioning improved the tube's performance. The pulse was of full length at a lower charge voltage. With the gradual increase in charge voltage, the pulse duration became erratic and sometimes shorter, until the tube becomes conditioned. A small frequency chirp was observed towards the end of shorter pulses. Performance improvement was noticed for a better vacuum. It required tens of shots to recondition the tube after an arcing has occurred. The electric field induced breakdown at the modulation and extraction section was identified as the primary cause of pulse shortening, not gap closure due to cathode plasma. Experimental results suggested the peak electric field must be kept below 150 kV/cm in the L-band tube to avoid pulse shortening. So, the grids were replaced by plates with "nosecone" aperture. This modification eliminated pulse shortening and attained 350 MW peak power with a maximum energy of 250 J per pulse.

• Miller has published a detailed experimental study of explosive emission from velvet cathode [Miller (1998)].

• Choi *et al.* have reported initial operation of the driving network, the cold test (simulation and experiment), and PIC simulation of a low voltage ultra-compact reltron designed by Titan/PSI for the University of New Mexico [Choi *et al.* (2001)]. X-ray shielding requirement was reported in a different publication [Kenyon (2001)]. i) The "UNM Reltron" is a low power version of high power commercial reltron. The reltron used a velvet cathode, driven by a PFN Marx generator comprised of four 30 kV, 0.22μF capacitors. The driving system was terminated by a dummy load of 770Ω for testing. It successfully produced 100 kV output voltage with approximately 1μS pulse duration with PRF 0.9-1.1 Hz. ii) The reltron modulation cavity was modeled in MAGIC, and resonant frequencies were obtained. The S_{11} was measured by using an HP8720 network analyzer in frequency sweep mode. The fundamental TM_{01} mode was excited in the cavity by end-stripped coaxial cables. The measured and simulation results matched closely. iii) A hot test simulation was conducted by modeling the full reltron tube. Initial simulation set-up with 100 kV, 1kA resulted in an immediate formation of the virtual cathode in front of the cathode, within 0.1 nS. The beam spread was brought down to a reasonable level by keeping the

beam current below 200 Amp. A high axial electric field was introduced to simulate the effect of postacceleration, but it did not reduce the beam spread. It was predicted that the numerical instability of the PIC code might be responsible for this unexpected result. So, driver voltage was increased to 180 kV with a moderate current of 400 A. This set-up resulted in an acceptable result. Though the simulation input voltage was higher than the actual source's capacity, the overall simulation provided an accurate picture of the modulation process.

• C. S. Kenyon of Army Research Laboratory (ARL) reported the requirement of X-ray shielding for reltron. Lead shell with 11 cm thickness was required for providing protection to the operator for exposure time less than 50 hours/year [Kenyon (2001)].

• Choi *et al.* published a characterization study of the pulsed power supply and the modulation section along with initial experimental hot test results [Choi *et al.* (2002)]. The educational reltron was designed for conducting pulsed power and HPM related experiments (output power of 10's of MW in S-band). There was a TM-to-TE mode converter at the output section. Possible grid damage (melting) due to failure in closing the crowbar switch (that terminates the voltage pulse) was discussed. B-dot and E-dot probes were used to excite the cavity with TM_{01} mode, and S_{12} was measured. The initial hot test demonstrated a beam current between 200-300 A and an impedance $\sim 500\Omega$. It was reported that the spectrum of the B-dot probe signal was inconclusive, and instrumentation modification was needed for improving the measurements [Choi *et al.* (2002)].

• Kim *et al.* have reported a PIC simulation work on a thermionic cathode based gridless reltron. A similar tube was reported by Miller *et al.* in 1995 (the extended lifetime design). The modeling procedure and simulation set-up for both the cold test and the hot test were explained in detail. The change in all three mode frequencies with coupling depth was reported. A single extraction cavity was used in this simulation. An output coupler was modeled by a ring-shaped conductor with finite conductivity (0.02 S/m). The conductivity was tuned for achieving a proper quality factor (90) of the extraction section. The hot test results were very promising. With respective beam voltage and postacceleration voltage of 120 kV and 800 kV, and beam current of 80 A, 38.3 MW radiated power

was generated with 52% efficiency. A focusing magnetic field of 1.4 kG was applied in simulation [Kim *et al.* (2009)].

• Soh *et al.* have reported the circuit model of reltron's modulation cavity and analytically derived the frequencies, and the currents in three normal modes [Soh *et al.* (2010)]. The cavity is represented by three inductively coupled loops consisting of series RLC circuits. The relation between the coupling coefficient and the mode frequencies revealed that 0 and π mode could be suppressed by increasing the coupling factor k. The frequency of 0 mode falls below cutoff, and it becomes imaginary for π mode with k. MAGIC simulation of the resonant modes was carried out. The simulation could not obtain the EM field pattern and the resonant frequency of 0 mode as it "did not converge".

• Soh *et al.* presented the single-particle analysis and PIC simulation of dual cavity reltron. A second cavity was used to increase beam modulation. Both the cavities were designed at the same resonant frequency of $\pi/2$ mode. The anode-cathode gap was driven by a 100 kV rectangular pulse with rising time 1 ns, and a similar pulse of 500 kV drove the postacceleration gap. The grid transparency was set to 97%. A total of 400 MW output power was observed from the two ports. The input power across the anode-cathode gap was 227 MW. Hence, power a gain of 1.76 was achieved [Soh *et al.* (2011)].

• In subsequent work, Soh *et al.* studied a dual-mode reltron through computer simulation. Two modes (TM_{010} and TM_{110}) were excited individually and simultaneously in the reltron's modulation cavity. In singe mode operation, a solid beam of radius 2.54 cm was used in TM_{010} mode, and an annular beam with outer and inner radius 3.91 cm and 3.17 cm, respectively, were used in TM_{110} mode. The iris was adjusted to tune the output cavity for successfully extracting the microwave power in each mode. Beam field interaction in the two individual modes produced 81 MW and 40.5 MW power with 23% and 17% efficiency at frequencies 2.395 GHz and 3.579 GHz, respectively. The output spectrum revealed power content in higher-order harmonics, as well. In dual-mode operation, a solid beam of 2.54 cm radius was used, and extraction cavities were tuned to fundamental and harmonic frequencies of each mode. The total power of 128 MW was generated with 35% efficiency when both the modes were excited together. That was greater than the sum

of total power generated in individual modes. It took longer time to saturate in dual-mode operation [Soh *et al.* (2012)].

• Mahto and Jain have derived the start oscillation current from the theory of self-modulation, and external modulation of the relativistic electron beam, in combination with discrete monotron oscillator. The design methodology was presented with a flowchart. A 5% difference in PIC simulation results were found with experimental work of [Miller *et al.* (1992)]. The oscillation condition was derived from the theory of relativistic klystron oscillator. Analysis of the bunching field, modulation process, and associated energy were presented [Mahto and Jain (2016)].

• In the next work, a detailed study of virtual cathode formation inside reltron's modulation cavity was performed through PIC simulation. The space charge limiting current and steady-state conditions were also derived [Mahto and Jain (2017)].

• A simulation study of low impedance reltron has demonstrated GW level power capability of reltron [Mahto and Jain (2019)].

• In recent years, a simulation study of thermionic emission based reltron has also been reported [Tripathi *et al.* (2020)].

A summary of experimental developments on reltrons is given in Table 1.1.

Table 1.1: Summary of experimental developments on reltrons

Reference	Peak power (MW)	Effi. (%)	Pulse duration (nS)	Energy/ pulse (J)	PRF (Hz)	Freq. (GHz)	Tuning range (% or GHz)
[Miller *et al.* 1992]	400	41.7	∼200	75-85	single shot	1	–
	200-250	40	∼300	60-75	single shot	3	–
	45	–	1000	25	single shot	3*	–
[Miller *et al.* 1994]	600	40.4	500-1000	>200	single shot	1	–
	>350	36.8	∼100	40	single shot	3	±5% of 3.04 GHz†
[Miller *et al.* 1995]	400	–	>1000	150	single shot	1.23	1.18-1.3
	100-700‡	–	–	–	1	0.75	0.75-0.95§
	20	40	5000¶	100	100‖	2.856	–
[Miller *et al.* 1998]	500	40	500	>200	<10	0.75	± 15%**
	400	–	∼1000††	300	–	0.75	–

1.4.3 Standpoint of Reltron

The peak power multiplied by the square of frequency (Pf^2) is a ranking parameter of a device's development and effectiveness in directed energy application. Reltron is shown in the Pf^2 graph shown in Figure 1.11 according to its specifications. It is a mildly relativistic HPM oscillator that does not suffer from pulse shortening, and mode competition, yet capable of repetitive pulse operation.

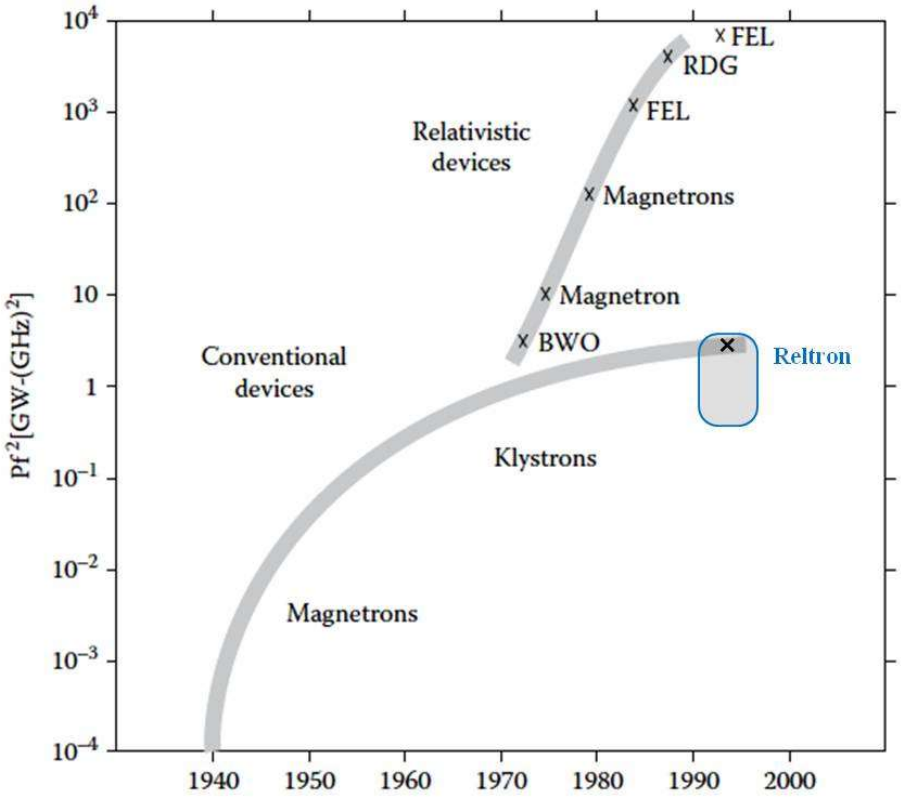

Figure 1.11: Growth of microwave devices in terms of Pf^2 [Benford *et al.* (2007)].

*3 GHz extraction section used with 1 GHz modulation section

†asymmetrical tuning by single-sided plunger

‡with three additional modulation cavities and two extraction cavities

§for the 0.75 GHz tube. Tubes covering 0.7-11 GHz were also developed for HPM effects testing

¶with brazed construction, ceramic insulator, Scandate thermionic cathode, gridless modulation section

‖500^{o}C bakeout, and hard vacuum (10^{-8}-10^{-7} Torr) required, tube length 19 inch and weight 80 pound

**double-sided plunger tuning mechanism for changing main cavity diameter

††grids of output cavities were replaced with nosecone design with 4.45 cm diameter

1.5 Motivation and Problem Definition

1.5.1 Motivation

The motivation for research on reltron is inspired by its unique features and potential application areas. Though it is a relatively new device, its foundation is set on well-known devices like LINAC, SCO, and klystron. Various experimental demonstrations have proved its capability as a megawatt-class HPM oscillator. It have advanced significantly in terms of output power and efficiency. Simultaneously it has demonstrated many additional features desirable from an HPM source like a compact form factor, high energy per pulse, easy power extraction, frequency stability, tunability, variable pulse duration, and repetition rate. Moreover, the reltrons are immune to fundamental limitations like pulse shortening, and mode competition, that are very common in most of the HPM sources. Sufficient experimental results are available that would help in setting benchmarks and in calibrating a simulation set-up to explore and predict further possibilities with high accuracy. So, the topic has been taken up with an aspiration to make some meaningful contribution in its advancement.

1.5.2 Problem definition

The following research gaps were identified after going through the literature –

- The design methodology of reltron has been reported, but the relations among the normal modes and the respective dimensional parameters of the the cavity modulation section is unclear.

- The equivalent circuit model of reltron's modulation section has been published, but the dispersion relation is not derived.

- 3D PIC simulations have been carried out, aiming to the improvement of output power and efficiency. The effects of relevant modulation section parameters on device performance and tunability are yet to be studied.

- Normal mode field patterns inside the modulation section reveal that the side cavity couples the other two. The possibility of performance improvement with more numbers of side cavities needs to be explored.

1.6 Plan and Scope

A detailed chapter plan is as follows –

Chapter 1 introduces the three fundamental types of radiation mechanisms, the classification of HPM sources, the origin of HPM technology, and the advancement of various HPM sources. A detailed literature review on reltron has been presented, which leads to the motivation of present work and the problem definition.

Chapter 2 presents the construction and working principle, parametric analysis of normal mode frequencies as a function of dimensional parameters, and cold-test of the modulation section. A modulation section was first analytically designed and then modeled in CST Microwave Studio (CST-MWS) and MAGIC. The obtained electromagnetic field patterns and frequencies in three lower-order normal modes matched from both the software packages. Thereafter, variations in mode frequencies were recorded by sequentially varying all the dimensional parameters within a range that considerably modifies the mode frequencies, without altering their order. In the process, the cavity dimensions were optimized for equal and maximum separation between the three modes. The S-parameter was also obtained through the Frequency-domain solver, and the quality factors and cavity reactances were calculated. Though the normal mode frequencies can accurately be predicted by simulation, they can not be measured directly inside a cavity with metallic boundary. However, the frequencies of S_{11} minima were found to match with that of the normal modes, which aid in an indirect measurement of the normal mode frequencies. A modulation section was constructed with the optimized cavity dimensions from a copper sheet, and the S- parameter was measured. The measured and simulated results matched with the good agreement. The modulation section's construction, measurement set-up, and the measured results are discussed in detail in this chapter. A brief description of the Eigenmode solver and the Frequency-domain solver are also included.

Chapter 3 covers the electromagnetic analysis leading to the dispersion relation of reltron's RF interaction structure. The equivalent circuit model of cavity resonator has been referred for its simplicity and accuracy. A set of circuit equations is formed, an rearranged as an eigenvalue problem. The solution gave the eigenvalues (oscillation frequencies) and the corresponding eigenvectors (relative direction of currents). The dispersion relation was derived thereafter from the generalized eigenvalue equations. Numerical simulations have been carried out to find the eigenvalues and the corresponding eigenvectors at different coupling depths. The coupling coefficient, specific to the designed modulation section, has been calculated.

Chapter 4 describes the simulation results of an S-band reltron. Particle-in-cell (PIC) solver of CST MWS was used for the simulation. One way of setting up the simulation for reproducing the original experimental work has been discussed. Reltron's operating frequency is tunable within a wide range by changing the main cavity diameter. A possibility of an additional tunability by varying idler disc length and efficiency enhancement by varying coupling depth has been reported. A brief description of the PIC solver is also included in the chapter.

Chapter 5 includes the performance improvement of the existing device. A double-side-cavity reltron is explored that demonstrated faster start-up of oscillation, leading to prolonged pulse duration and higher energy per pulse. Simulation results predicted that the dual cavity extraction section could be successfully utilized in this kind of reltron, as well.

In **Chapter 6**, previous chapters are summarized to conclude the thesis, and the limitations of the present study are discussed to outline the possibilities for future work.

1.7 Conclusion

The technology development trends in various HPM tubes have been studied and summarized. The topic is narrowed down to the highly efficient, compact, and versatile HPM oscillator - reltron. A detailed literature review has been carried out to comprehend the device and identify a few research problems. A course of action has been planned, and the chapters are structured accordingly in the form of the present dissertation.

CHAPTER ii

Parametric Study of Normal Mode Frequencies and Cold-test Results[†]

Chapter index

2 Parametric Study of Normal Mode Frequencies and Cold-test Results 35

2.1 Introduction 35
2.2 Concept of the Design 36
2.2.1 Beam injector 36
2.2.2 Modulation section 37
2.2.3 Postacceleration section 40
2.2.4 Extraction section 40
2.3 Working Principle 40
2.4 Attractive Features 41
2.5 Mode Designation 42
2.5.1 Eigenmode solver 44
2.6 Parametric study of Normal Mode Frequencies 45
2.7 Simulation of S-parameter 46
2.7.1 Frequency-domain solver 48
2.8 Calculation of Quality-factor and Cavity Reactance 49
2.9 Construction of a Test-cavity and S_{11} Measurement 51
2.9.1 Construction of test-cavity 51
2.9.2 Cold-test results 52
2.10 Conclusion 53

[†]Part of this work has been published as: S. Shee, and S. Dwivedi, "Cold-test of reltron modulation section and PIC simulation study on output power and efficiency," *Int. J. RF Microw Comput Aided Eng.*, vol. 30, no. 3, doi:10.1002/mmce.22103